Bulgarian Chemical Communications, Volume 46, Number 4 (pp. 680 – 686) 2014

A computational study on the smallest exohedrally functionalized fullerenes, $C_{20}X_8$ (X = H, F, Cl, Br, NH_2, OH and CN)

F. Naderi *

Department of Chemistry, Shahr-e-Qods Branch, Islamic Azad University, Tehran, Iran

Received August 9, 2013; Revised June 19, 2014

The structural stability and the electronic properties of $C_{20}X_8$ exohedrally functionalized fullerenes where X = H, F, Cl, Br, NH_2, OH and CN are probed at the B3LYP level of theory. Vibrational frequency calculations show that all systems are true minima. The calculated binding energies of exohedrally functionalized fullerenes show $C_{20}(CN)_8$ followed by $C_{20}F_8$ as the most stable exohedrally functionalized fullerenes by the binding energies of 6.628 and 5.484 eV, respectively. All exohedral derivatives decrease the conductivity of fullerene through increasing their HOMO-LUMO gap and therefore enhance their stability against electronic excitations. High charge transfer on the surfaces of our stable exohedrally functionalized fullerenes, especially $C_{20}(OH)_8$ provokes further investigations on their possible application for hydrogen storage.

Keywords: Hybrid density functional theory (B3LYP); HOMO and LUMO; Exohedrally functionalized; $C_{20}X_8$; DFT.

INTRODUCTION

The discovery of C_{60} [1,2] was followed by the synthesis of other members of the fullerene family including the smallest possible fullerene cage, i.e. C_{20} [3]. The thermodynamic stability of C_{20} is different from that of C_{60} because of its extreme curvature and reactivity as it is composed of 12 pentagons and no hexagons. The angle between two adjacent bonds is 108º, much smaller than the optimal sp^2 angle of carbon, which is 120º. Therefore, it is a very strained structure. However, the fullerenes suffering from adjacent pentagons can be stabilized by forming endohedral (where the dopant is inside the cage) or exohedral (where the dopant is outside or between fullerene cages) derivatives with other groups [4]. Endohedral doping proved to be applicable in successful synthesis of $Sc_2@C_{66}$ [5], $Sc_2C_2@C_{68}$ [6], and $Sc_3N@C_{68}$ [7]. In the case of small cages, Moran *et al*. studied the equilibrium geometries and frequencies of endohedral complexes $X@C_{20}H_{20}$ where X = H, He, Ne, Ar, Li, Li^+, Be, Be^+, Be^{2+}, Na, Na^+, Mg, Mg^+ and Mg^{2+} [8]. Shakib et al. [9] found that minima fullerenes $Li^+@C_{20}H_{20}$ and $Mg^{2+}@C_{20}H_{20}$ are more stable than their isolated components. Recently, we carried out a similar study on $X@C_{12}Si_8$ complexes where X = Li^+, Na^+, K^+, Be^{2+}, Mg^{2+}, Ca^{2+}, Al^{3+}, and Ga^{3+}. The calculated binding energies showed the stabilization of $C_{12}Si_8$ through the inclusion of Be^{2+}, Mg^{2+}, Al^{3+}, and Ga^{3+}. On the other hand, the structures and electronic properties of exohedral complexes have been also of interest. $C_{54}Cl_8$ [10], $C_{56}Cl_8$, $C_{56}Cl_{10}$ [11], $C_{56}Cl_{10}$ [12], $C_{58}X_{18}$ (X = H, F and Cl) [13], hept-$C_{62}X_2$ [14], $C_{64}X_4$ [15], and $C_{66}X_4$ (X = H, F, Cl, or Br) [16] were explored using the density functional theory. The first exohedral fullerene $C_{50}Cl_{10}$ [17] was synthesized in 2004 by Xie *et al*., followed by the synthesis of $C_{64}H_4$ [18] and $C_{64}Cl_4$ [19]. Now, what about small fullerenes? How does exohedral doping affect the stability of the smallest fullerene cage C_{20}? In this manner, we focused our calculations on $C_{20}X_8$ exohedrally functionalized fullerenes where X = H, F, Cl, Br, NH_2, OH and CN to probe the applicability of exohedral doping in stabilization of C_{20}. The substituents are attached to eight symmetric positions of the cage in a case that none of them are adjacent to each other.

COMPUTATIONAL METHODS

Full geometry optimizations are accomplished by means of hybrid functional B3LYP [20-22] and the 6-31+G* basis set, as implemented in Gaussian 03 [23]. The applied basis set is comprised of Pople's well known 6-31G* basis set [24,25] and an extra plus due to the importance of diffuse functions [26,27]. Vibrational frequency computations confirm that the fully optimized structures are indeed minima (NIMAG = 0). To obtain more accurate energetic data, single point calculations are performed at B3LYP/6-311++G**

* To whom all correspondence should be sent:
E-mail: fnaderi2@yahoo.com

level. As a stability criterion of different configurations, binding energy per atom is calculated according to the following expression [28]:

$$E_b = (20E_C + 8E_X – E)/n$$

where E is the total energy of the $C_{20}X_8$ exohedrally functionalized fullerenes and Ex for NH_2, OH and CN groups is equal to the sum of energy of their elements. Systems with larger binding energies are more stable. The electronic conductivity of the exohedrally functionalized fullerenes which is related to the HOMO-LUMO energy gaps were calculated at B3LYP/6-311++G**.

The nucleophilicity index, N, which was introduced by Domingo *et al.* [29], is calculated as $N = E_{HOMO(Nu)} - E_{HOMO(TTFE)}$, where tetrakis tetrafluoroethylene (TTFE) is chosen as the reference. The global electrophilicity, ω [30], is also calculated following the expression, $\omega = (\mu 2/2\eta)$, where μ is the chemical potential ($\mu \approx (EHOMO + ELUMO)/2$) and η is the chemical hardness ($\eta = ELUMO - EHOMO$) [31]. NBO population analysis on optimized structures is also accomplished at the same level [32].

RESULTS AND DISCUSSION

Following the successful synthesis of dodecahedrane $C_{20}H_{20}$, a large number of exohedral derivatives of fullerene C_{20} have been synthesized with dodecahedrane as starting point. Among various exohedral derivatives of C_{20}, of particular interest are the polyunsaturated dodecahedranes $C_{20}R_n$ (n = 18, 16, 14, 12, 10; R = H or other substituents) that have one to five highly bent unsaturated C=C bonds [33]. In this work first full geometry optimizations of various exohedral derivatives of C_{20} ($C_{20}H_{10}$, $C_{20}H_{12}$, $C_{20}H_{14}$a and $C_{20}H_{14}$b), (their figures are represented in supporting information) are performed and binding energy per atom is calculated. The binding energies are 5.19, 5.09, 5.21 and 5.22 eV/atom, respectively, while the binding energy of $C_{20}H_8$ is 5.44eV/atom. Then eight symmetrical positions of C_{20} are selected for evolution of $C_{20}X_8$ fullerenes where X = H, F, Cl, Br, NH_2, OH and CN (Figure 1).

The smallest fullerene that satisfies Euler's theorem is C_{20} which is highly strained as a result of the extreme pyramidalization of the double bonds. Eight symmetrical positions of this fullerene are selected to have maximum double bond without any extra strain to have the most relative stabilities of $C_{20}X_8$.

Geometry optimizations and the resulted binding energies

The optimized geometries of C_{20} and its analogues (Figure 1) in the gas phase are listed in Table 1. Dodecahedral fullerene C_{20} does not adopt the perfect I_h symmetry due to Jahn-Teller distortion, whereas its lowest energy form is still in dispute [34-35]. The work by Chen *et al*. demonstrates that all five possible isomers of C_{20} (C_2, C_{2h}, C_i, D_{3d} and D_{2h} symmetries) are isoenergetic (within 0.2 kcal/mol at B3LYP/6-31G*, and within 0.5 kcal/mol at MP2/6-31G*) and have essentially the same structural parameters at both B3LYP and MP2 levels [36]. The C=C bond lengths of C_i symmetry C_{20} are 1.445 Å, which is close to the sum of covalent radii of two C atoms (C: 0.76 Å). The obtained structure of C_{20} is in excellent agreement with that computed by Chen *et al.* [37].

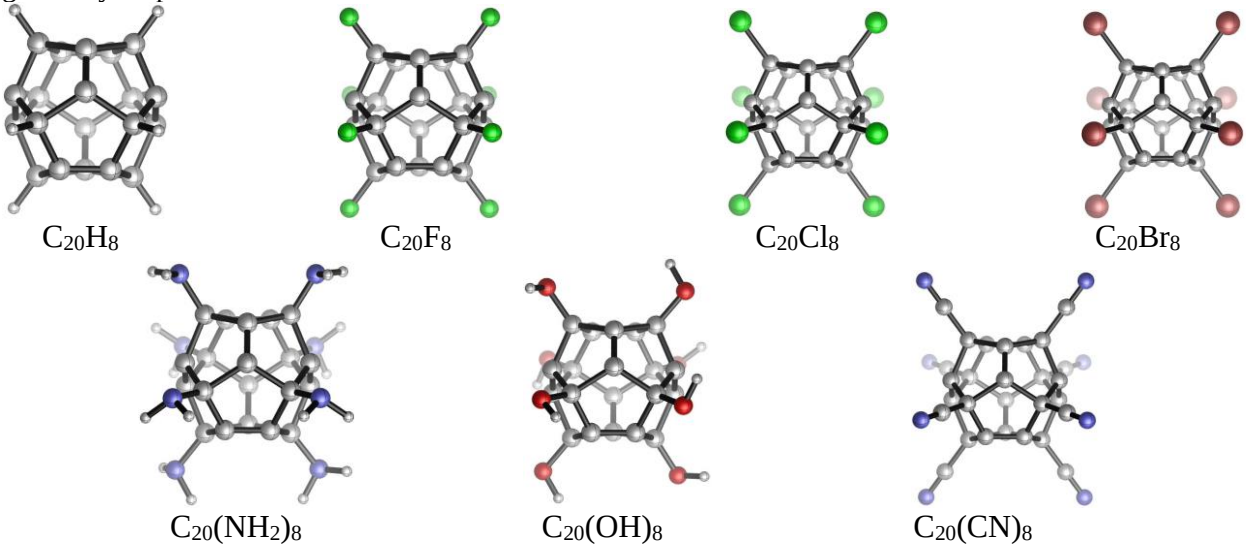

Fig. 1. Optimized heterofullerenes at B3LYP/6-31+G*.

Table 1. Point groups (PG), total energies (E_{tot} in a.u.), ranges of C=C and X–C bond lengths (Å) and C–C–X angles (º) for the scrutinized heterofullerenes along with C_{20} at the B3LYP/6-31+G* level.

Species	PG	E_{tot} (a.u.)	C–C	C=C	X–C	C–C–X
C_{20}	C_i	-761.6019944	1.400-1.536		-	-
$C_{20}H_8$	T_h	-766.7585347	1.540	1.352	1.093	118.81
$C_{20}F_8$	T_h	-1560.8726881	1.534	1.353	1.373	118.18
$C_{20}Cl_8$	T_h	-4443.7128301	1.531	1.351	1.797	118.60
$C_{20}Br_8$	T_h	-21355.0790532	1.525	1.351	1.960	118.36
$C_{20}(NH_2)_8$	C_1	-1209.4094692	1.537-1.555	1.350-1.353	1.449-1.454	116.64-123.86
$C_{20}(OH)_8$	C_1	-1368.6929686	1.544	1.352	1.404	120.72
$C_{20}(CN)_8$	T_h	-1504.7670055	1.546	1.344	1.160	119.28

Introducing H atoms to C_{20} upgrades its symmetry from C_i to T_h. This is along with the uniformity of bond lengths in $C_{20}H_8$. The range of 1.400-1.536 Å C=C bonds of C_{20} is replaced with single bonds of 1.540 Å and double bonds of 1.352 Å, pretty close to typical $H_3C–CH_3$ and $H_2C=CH_2$ bonds. The H–C bond length of 1.093 Å is also completely close to a typical $H–CH_3$ bond length of 1.094 Å (Table 1).

Evidently, the presence of the eight sp^3 carbon atoms extinguishes the electron delocalization on the surface of the cage. The same structural features are observed for all other species. However, $C_{20}(NH_2)_8$ does not show a fixed length for each of the single and double bonds but a narrow range. This is because it obeys C_1 symmetry instead of T_h. Although the cage of $C_{20}(OH)_8$ is itself T_h, the overall structure obeys C_1 symmetry due to the different spatial orientations of hydroxyl groups. While all species show C=C bond lengths of 1.350-1.353 Å, those of $C_{20}(CN)_8$ are noticeably shorter (1.344 Å) due to both inductive and mesomeric electron withdrawing of cyano groups (Table 1).

As stated by Hoffmann, Schleyer, and Schaefer, talking about the stability of a species necessitates that not only the obligatory vibrational analysis demonstrating all frequencies real, but also the computed smallest vibrational frequency (ν_{min}) should be reasonably large, i.e. more than 100 cm^{-1} [38]. Interestingly, ν_{min} increases from 32 cm^{-1} in C_{20} to 474 cm^{-1} in $C_{20}H_8$. This is because eight strained sp^2 carbon atoms are replaced with the strain-free sp^3 atoms. Halogenated fullerenes show lower frequencies but those of $C_{20}F_8$ and $C_{20}Cl_8$ are still larger than 100 cm^{-1}. The ν_{min} of $C_{20}Br_8$ is 61 cm^{-1} showing the weakness of C–Br bonds. While the ν_{min} of $C_{20}(NH_2)_8$ and $C_{20}(OH)_8$ bearing π-electron donor groups are satisfactorily large, the ν_{min} of $C_{20}(CN)_8$ with π-electron acceptor group is lower than 100 cm^{-1} (Table 2).

Table 2. Binding energies per atom (B.E./atom) at B3LYP/6-311++G** and smallest vibrational frequencies (ν_{min}) for the scrutinized heterofullerenes along with C20 at B3LYP/6-31+G*.

Species	B.E./atom (eV)	ν_{min} (cm^{-1})
C_{20}	6.063	32
$C_{20}H_8$	5.437	474
$C_{20}F_8$	5.484	192
$C_{20}Cl_8$	5.085	108
$C_{20}Br_8$	4.944	61
$C_{20}(NH_2)_8$	5.252	157
$C_{20}(OH)_8$	5.148	182
$C_{20}(CN)_8$	6.628	85

The IR vibrational frequencies are computed to further provide the distinctive spectroscopic fingerprints of these probably accessible fullerenes. The simulated IR vibrational spectra of the fullerenes are illustrated in Fig.2, suggesting the prominent peaks.

These IR signatures provide useful information for their future experimental detections. It should be stressed at the outset that theoretical frequencies are almost universally overestimated compared to experimental results, even for more accurate methods, such as MP2, CCSD. It is not our intention in this study to predict absolute values of frequencies, but rather to seek for patterns in the data which might help to identify different forms of $C_{20}X_8$ fullerenes.

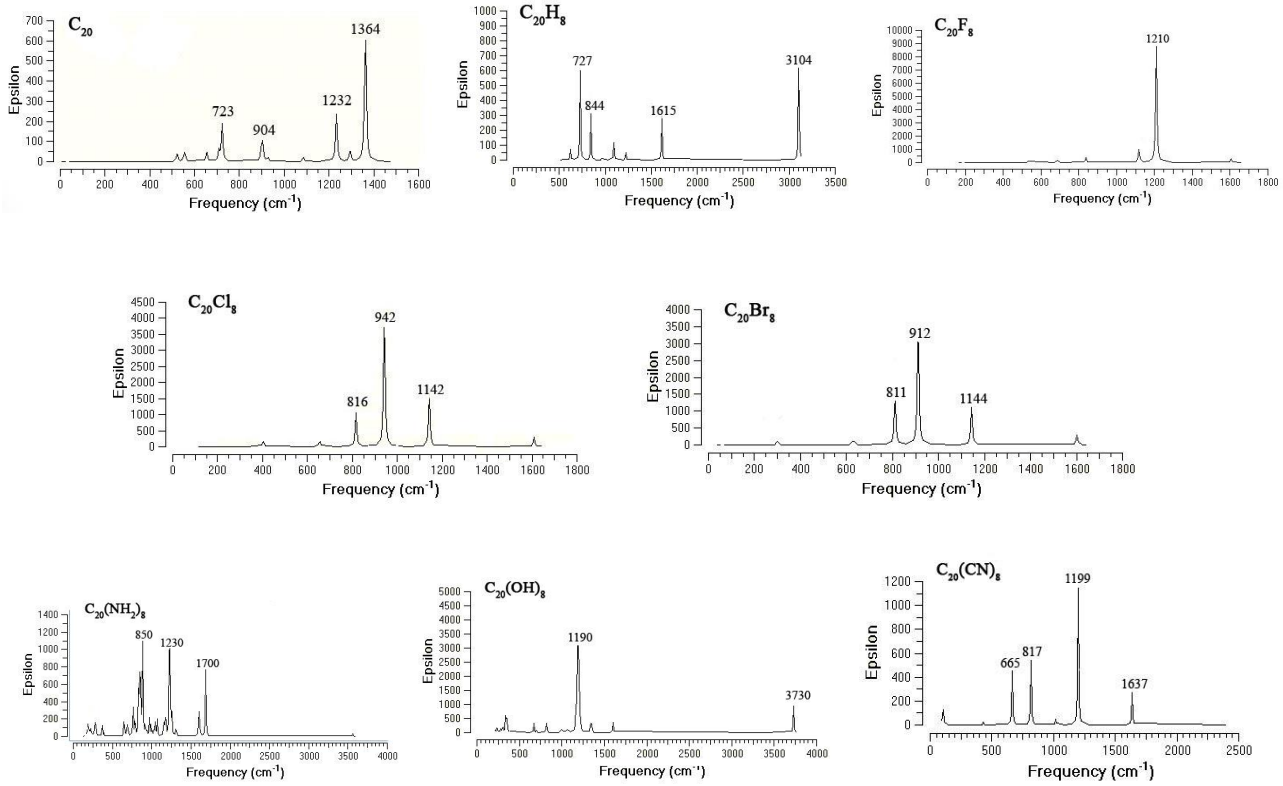

Fig. 2. Calculated IR spectra of $C_{20}X_8$ heterofullerenes at B3LYP/6-31+G*.

The binding energy of $C_{20}H_8$ is 5.437 eV which is less than that of C_{20} (6.063 eV) due to the absence of C=C bonds. From $C_{20}F_8$ to $C_{20}Br_8$ one finds a decreasing trend in binding energy due to the weakness of C–Br bonds compared to C–Cl ones and C–Cl compared to C–F. This is along with the decreasing trend of ν_{min} among halogenated fullerene derivatives. The interesting point is the enormous stability of the fullerene bearing π-electron withdrawing group i.e. CN. The binding energy of $C_{20}(CN)_8$ is 6.628 which the highest value of all studied fullerene derivatives, consistent with the structural features (Table 2). In order to further provide distinctive spectroscopic fingerprints of probably accessible $C_{20}X_8$ fullerene derivatives, their calculated IR spectra are depicted in Figure 2.

$C_{20}X_8$ exohedrally functionalized fullerenes through NBO atomic charges

It was shown that point charges on the material's surface can improve the hydrogen storage capacity since they increase the binding energy of hydrogen [39-42]. The NBO population analysis on optimized structures is accomplished at the B3LYP/6-311++G**//B3LYP/6-31+G*.

The carbon atoms of sole fullerene bear varying charges from –0.050 to +0.050. In contrast, the structural uniformity of $C_{20}H_8$ is along with the electronic uniformity as all sp^3 carbons carry a negative charge of –0.283 while the more electronegative sp^2 carbons carry a positive charge of +0.034. Electronegative fluoro substituent induces an overall electron density transfer and remains positively charged sp^2 and sp^3 carbons. On the other hand, electron donating characteristics of Cl and Br results in the negatively charged sp^3 carbons, i.e. this time the electron density transfer is from the exohedral substituents to the fullerene cage. Generally, since electronegativity decreases down a group of the periodic table, in $C_{20}F_8$, $C_{20}Cl_8$ and $C_{20}Br_8$, a considerable charge transfer occurs from them to the remaining carbon atoms of the cage. According to the calculated NBO atomic charges, the negative charges on F atoms are –0.354 while the charges on C atoms range from +0.033 to +0.304. The positive charges on Cl and Br atoms of $C_{20}Cl_8$ and $C_{20}Br_8$ are +0.025 and +0.094 while the charges on C atoms range from –0.131 to +0.058 and –0.194 to +0.075, respectively. Considering both stability and charge distribution on the surfaces of $C_{20}F_8$, $C_{20}Cl_8$ and $C_{20}Br_8$, it seems that $C_{20}F_8$ is possibly the best candidate for hydrogen storage.

Hydrogen and carbon atoms in $C_{20}H_8$ and $C_{20}(CN)_8$ carry a positive charge, i.e. +0.232 for H and +0.276 for C (Table 3).

Table 3. Ranges of NBO atomic charges of carbon (C) and exohedral derivatives (X) for $C_{20}X_8$ heterofullerenes along with C_{20} at B3LYP/6-311++G**//B3LYP/6-31+G*.

Species	C_{sp3}	C_{sp2}	X[a]	Y[b]
C_{20}	-	(–0.050) - (+0.050)	-	-
$C_{20}H_8$	–0.283	+0.034	+0.232	-
$C_{20}F_8$	+0.304	+0.034	–0.354	-
$C_{20}Cl_8$	(–0.111) - (–0.131)	(+0.053) - (+0.080)	+0.026	-
$C_{20}Br_8$	(–0.176) - (–0.198)	(+0.049) - (+0.076)	(+0.094) - (+0.095)	-
$C_{20}(NH_2)_8$	(–0.073) - (+0.046)	(–0.016) - (+0.064)	(–0.816) - (–0.869)	(+0.349) - (+0.362)
$C_{20}(OH)_8$	(+0.188) - (+0.197)	(+0.007) - (+0.075)	(–0.703) - (–0.718)	(+0.467) - (+0.470)
[c]$C_{20}(CN)_8$	–0.221	+0.112	+0.276	–0.224

[a] O in $C_{20}(OH)_8$, C in $C_{20}(CN)$ and N in $C_{20}(NH_2)_8$
[b] H in $C_{20}(OH)_8$ and $C_{20}(NH_2)_8$, and N in $C_{20}(CN)_8$
[c] All cyano groups bear the same charges except one, the carbon and nitrogen of which bear the relative charges of +0.294 and +0.232, respectively.

The differences between their positive charges correlate with the differences between their electronegativities. However, the difference of ~ 0.350 between the electronegativities of H and C, cannot simply explain the considerable difference between their positive charges. Eventually, $C_{20}(OH)_8$ with –0.711 charged O and +0.197 charged C shows the highest charge separation on its surface leading to one of the highest binding energies and hence a possible candidate for hydrogen storage.

HOMO-LUMO gaps, nucleophilicity and electrophilicity of exohedrally functionalized fullerenes

The electrons donated by a molecule in a reaction should be from its HOMO, while the electrons captured by the molecule should locate on its LUMO. Furthermore, the atom on which the HOMO mainly distributes should have the ability for detaching electrons, whereas the atom with the occupation of the LUMO should gain electrons [26]. On this basis, the HOMO–LUMO gap is traditionally associated with chemical stability against electronic excitation, with larger gap corresponding to greater stability. Note that pyramidalization of a unsaturated C=C bond remarkably reduces its energy gap between the π (bonding) and π * (antibonding) molecular orbitals, leading to "diradical" character and, of course, much higher reactivity. The HOMO-LUMO gap of exohedrally functionalized fullerenes varies depending on the type of exohedral derivative atoms. All exohedral derivatives increase the gap leading to the enhanced stability against electronic excitations. Specifically, $C_{20}H_8$, and $C_{20}(OH)_8$ show significant stabilities with gaps of 5.670 and 5.604 eV, respectively. Interestingly, based on N and ω indices, C_{20} is both the most nucleophilic and electrophilic species among all studied fullerenes and has a very small HOMO-LUMO gap (1.899 eV) (Table 4).

This clearly represents its huge instability resulting from extreme curvature as said before. The nucleophilicity and electrophilicity of C_{20} is greatly influenced by substitution. After C_{20}, expectedly,

Table 4. HOMO and LUMO energies, HOMO-LUMO energy gaps (ΔEH-L), nucleophilicity (N) and electrophilicity (ω) indices for the scrutinized heterofullerenes along with C_{20} at B3LYP/6-311++G**//B3LYP/6-31+G*.

Species	HOMO (a.u.)	LUMO (a.u.)	$\Delta E_{H\text{-}L}$ (eV)	N (eV)	ω (eV)
C_{20}	-0.20339	-0.13361	1.899	4.798	5.536
$C_{20}H_8$	-0.24902	-0.04065	5.670	3.556	1.370
$C_{20}F_8$	-0.31844	-0.13047	5.115	1.667	3.646
$C_{20}Cl_8$	-0.30309	-0.11703	5.063	2.085	3.227
$C_{20}Br_8$	-0.29229	-0.11791	4.745	2.379	3.282
$C_{20}(NH_2)_8$	-0.23261	-0.05123	4.936	4.003	1.511
$C_{20}(OH)_8$	-0.26679	-0.08001	5.082	3.073	2.190
$C_{20}(CN)_8$	-0.36080	-0.15484	5.604	0.515	4.391
TTFE	-0.37971	-0.14198	6.469	0.000	3.894

$C_{20}(CN)_8$ with *N* and ω values of 0.515 and 4.391 eV, respectively, is the least nucleophilic and the most electrophilic species (Table 4). Eventually, based on Pauling electronegativities, NH_2 is more nucleophilic than OH and Cl more than F.

CONCLUSION

The smallest possible fullerene cage, i.e. C_{20}, is taken into account of exohedral derivatives through our previously reported isolation strategy. The exohedral derivative atoms are replaced at eight selected symmetric positions of C_{20}. Probing exohedrally functionalized fullerenes $C_{20}X_8$ where X = H, F, Cl, Br, NH_2, OH and CN reveals that all these systems are true minima. Calculated binding energy of 6.628 eV shows $C_{20}(CN)_8$ as the most stable exohedrally functionalized fullerene followed by $C_{20}F_8$ with the binding energy of 5.484 eV. The binding energies of the other exohedrally functionalized fullerenes ranges from 4.944 to 5.437 eV. Exohedral derivatives lead to a high charge distribution on the surfaces of all exohedrally functionalized fullerenes with the highest distribution on $C_{20}(OH)_8$ with +0.197 charged carbons and –0.711 charged O atoms. These high point charges upon the exohedrally functionalized fullerenes surface can improve the storage capacity and make them worthy of investigation for hydrogen storage. All exohedral derivatives increase the HOMO-LUMO gap leading to enhanced stability against electronic excitations. Also, all exohedrally functionalized fullerenes have lower nucleophilicity and electrophilicity than C_{20} indicating their stability compared to the unsubstituted cage.

REFERENCES

1. D.A. Bochvar, E.G. Gal'perin, *Proc. Acad. Sci. USSR*, 209, 239 (1973).
2. H.W. Kroto, J.R. Health, S.C. O'Brien, R.F. Curl, R.E. Smalley, *Nature*, 318, 162 (1985).
3. H. Prinzbach, A. Weller, P. Landenberger, F. Wahl, J. Worth, L.T. Scott, M. Gelmont, D. Olevano, B.V. Issendorff, *Nature*, 407, 60 (2000).
4. (a) L. Türker, *Journal of Molecular Structure*: *THEOCHEM*, 593, 149 (2002). (b) L. Türker, *Journal of Molecular Structure: THEOCHEM*, 624, 233 (2003).
5. C.R. Wang, T. Kai, T. Tomiyama, T. Yoshida, Y. Kobayashi, E. Nishibori, M. Takata, M. Sakata, H. Shinohara, *Materials science: Nature* ,408, 426 (2000).
6. Z.Q. Shi, X. Wu, C.R. Wang, X. Lu, H. Shinohara, *Angew. Chem. Int. Ed*., 45, 2107 (2006).
7. S. Stevenson, P.W. Fowler, T. Heine, J.C. Duchamp, G. Rice, T. Glass, K. Harich, E. Hajdu, R. Bible, H.C. Dorn, *Nature*, 408, 427 (2000).
8. (a) D. Moran, F. Stahl, E.D. Jemmis, H.F. Schaefer III, P.v.R. Schleyer, J. Phys. Chem. A ,106, 5144 (2002). (b) Z. Chen, H. Jiao, D. Moran, A. Hirsch, W. Thiel, P.v.R. Schleyer, *J. Phys. Chem.* A ,107, 2075 (2003).
9. F.A. Shakib, M.R. Momeni, 406,1471 (2011) .
10. X.F. Gao, Y.L. Zhao, *J. Comput. Chem*., 28,795 (2007).
11. D.L. Chen, W.Q. Tian, J.K. Feng, C.C. *Chem. Phys. Chem.*, 8, 2386 (2007).
12. Yuan-Zhi Tan, Xiao Han, Xin Wu, Ye-Yong Meng, Feng Zhu, Zhuo-Zhen Qian, Zhao-Jiang Liao,Ming-Hui Chen, Xin Lu, Su-Yuan Xie, Rong-Bin Huang, and Lan-Sun Zheng, *J. Am. Chem. Soc.* 130, 15240 (2008).
13. D. L. Chen; W. Q.Tian; J. K.Feng; C. C.Sun , *J. Phys. Chem. B* ,111, 5167 (2007).
14. L.L. Sun, S.W. Tang, Y.F. Chang, Z.L. Wang, R.S. Wang, *J. Comput. Chem*. 29, 2631 (2008).
15. Q.B. Yan, Q.R. Zheng, G. Su, *J. Phys. Chem*. C, 111, 549 (2007).
16. Q.B. Yan, Q.R. Zheng, G. Su, *Carbon*, 45, 1821 (2007) .
17. S.Y. Xie, F. Gao, X. Lu, R.B. Huang, C.R. Wang, X. Zhang, M.L. Liu, S.L. Deng, L.S. Zheng, *Science*, 304, 699 (2004).
18. C.R. Wang, Z.Q. Shi, L.J. Wan, X. Lu, L. Dunsch, C.Y. Shu, Y.L. Tang, H. Shinohara, *J. Am. Chem. Soc*.,128, 6605 (2006) .
19. X. Han, S.J. Zhou, Y.Z. Tan, X. Wu, F. Gao, Z.J. Liao, R.B. Huang, Y.Q. Feng, X. Lu, S.Y. Xie, L.S. Zheng, *Angew. Chem., Int. Ed*., 47, 5340 (2008).
20. A.D. Becke, *Phys. Rev. A*, 38, 3098 (1988).
21. A.D. Becke, *J. Chem. Phys*., 98, 5648 (1993) .
22. C. Lee, W. Yang, R.G. Parr, *Phys. Rev. B* ,37,758 (1988) .
23. M.J. Frisch, et al. Gaussian 03; Revision B.02, Gaussian, Inc.: Pittsburgh, PA, (2003). See the Supporting Information for the full reference.
24. P.C. Hariharan, J.A. Pople, *Mol. Phys.* ,27,209 (1974.
25. M.M. Francl, W.J. Pietro, W.J. Hehre, J.S. Binkley, M.S. Gordon, D.J. DeFrees, J.A. Pople, *J. Chem. Phys*. ,77, 3654 (1982.
26. T. Clark, J. Chandrasekhar, G.W. Spitznagel, P.v.R. Schleyer, *J. Comput. Chem*., 4, 294 (1983).
27. M.J. Frisch, J.A. Pople, J.S. Binkley, *J. Chem. Phys*., 80, 3265 (1984).
28. M.R.Momeni, F.A.Shakib, *J. Chem. Phys. Letters*, 492, 137 (2010).
29. L.R. Domingo, E. Chamorro, P. Pérez, *J. Org. Chem*.,73, 4615 (2008).
30. R.G. Parr, L. Szentpaly, S. Liu, *J. Am. Chem. Soc*., 121, 1922 (1999).
31. (a) R.G. Parr, R.G. Pearson, *J. Am. Chem. Soc*., 105, 7512 (1983). (b) R.G. Parr, W. Yang, Density Functional Theory of Atoms and Molecules, Oxford University Press: New York, NY, (1989).
32. E.D. Glendening, A.E. Reed, J.E. Carpenter, F. Weinhold, NBO Version 3.1.

33. (a) H.Prinzbach, *Angew. Chem., Int. Ed*. Engl., 32, 1722 (1993). (b) H. Prinzbach, K. Weber, *Angew. Chem., Int. Ed*. Engl., 33, 2239 (1994). (c) M. Bertau, F.Wahl, A.Weiler, K.Scheumann, J.Wörth, M. Keller, H.Prinzbach, *Tetrahedron*, 53, 10029 (1997).
34. A. Hirsch, Z. Chen, H. Jiao, *Angew. Chem., Int. Ed*. 39, 3915, (2000).
35. Z. Chen, T. Heine, H. Jiao, A. Hirsch, W. Thiel, P.v. R. Schleyer, *Chem. Eur. J.* ,10, 963 (2004).
36. A.K. Ott, G.A. Rechtsteiner, C. Felix, O. Hampe, M.F. Jarrold, R.P.V. Duyne, K. Raghavachari, *J. Chem. Phys*.,109, 9652 (1998).
37. X. Lu ,Z. Chen , *Chem. Rev*., 105, 3643 (2005).
38. R. Hoffmann, P.v.R. Schleyer, H.F. Schaefer *Angew. Chem. Int. Ed*., 47, 7164(2008).
39. G.E. Froudakis, *Nano Lett*., 1, 531 (2001.
40. M. Menon, E. Richter, A. Mavrandonakis, G. Froudakis, A.N. Andriotis, *Phys. Rev. B*, 69, 115322 (2004).
41. A. Mavrandonakis, G.E. Froudakis, M. Schnell, M. Muhlhauser, *Nano Lett*.,3, 1481 (2003).
42. G. Mpourmpakis, G.E. Froudakis, G.P. Lithoxoos, J. Samios, Carbon nanoscrolls: *Nano Lett*. 6, 1581(2006).

ЧИСЛЕНО ИЗСЛЕДВАНЕ НА НАЙ-МАЛКИТЕ ЕКСОЕДРИЧНИ ФУНКЦИОНАЛИЗИРАНИ ФУЛЕРЕНИ, $C_{20}X_8$ (X = H, F, Cl, Br, NH_2, OH И CN)

Ф. Надери*

Департамент по химия, Клон Шакх-е-Оодс,Ислямски университет „Асад“, Техеран, Иран

Постъпила на 9 август, 2013 г.; Коригирана на 19 юли 2014 г.

(Резюме)

Изпитани са структурната стабилност и електронните свойства на ексоедрични функционализирани фулерени $C_{20}X_8$, където X = H, F, Cl, Br, NH_2, OH и CN с помощта на B3LYP-ниво на теорията. Изчислените вибрационни честоти показват, че всички системи имат истински минимуми. Изчислените енергии на свързване за ексоедричните функционализирани фулерени показват, че $C_{20}(CN)_8$ и след него $C_{20}F_8$ са най-стабилните с енергии на свързване съответно 6.628 и 5.484 eV. Всички ексоедрични производни намаляват проводимостта на фулерените чрез нарастването на техните HOMO-LUMO области и затова повишават тяхната стабилност срещу електронно възбуждане. Високият пренос на заряда на повърхността на нашите стабилни ексоедрични функционализирани фулерени, особено $C_{20}(OH)_8$ предизвиква следващи изследвания върху техните възможности за складиране на водород.